

Thermodynamic properties of QCD with two flavors of Wilson-type lattice quarks *

Kazuyuki Kanaya^aMCSJ Institute of Physics, University of Tsukuba, Tsukuba, Ibaraki 305-8571, Japan for the CP-PACS Collaboration

^a[

I report on a study of finite temperature QCD by the CP-PACS Collaboration toward a precise determination of the equation of state with dynamical u,d quarks. Based on a systematic simulation using improved Wilson-type quarks on lattices with temporal size $N_t = 4$ and 6, the energy density and pressure are calculated as functions of temperature and renormalized light quark mass in the range $T/T_c \approx 0.7$ –2.5 and $m_{PS}/m_V = 0.65$ –0.95. Results for $N_t = 4$ are found to contain significant scaling violations, while results for $N_t = 6$ are suggested to be not far from the continuum limit. On the other hand, the quark mass dependence in the EOS turned out to be small for $m_{PS}/m_V \lesssim 0.8$.

1. INTRODUCTION

Theoretical understanding on the nature of the finite temperature QCD phase transition and its thermodynamic properties is indispensable in extracting an unambiguous signal of quark-gluon plasma production from heavy-ion collision experiments. In particular, the equation of state (EOS) of quark-gluon plasma belongs to the most basic information needed. Here, numerical simulations of lattice QCD provides us with the only systematic way to calculate these quantities directly from the first principles of QCD [1].

In this paper, I present our study of finite temperature QCD on the lattice with dynamical u and d quarks, focusing on the efforts toward a precise determination of the EOS [2,3]. Calculations are made on the CP-PACS computer, a dedicated parallel computer developed at the University of Tsukuba in 1996 by physicists and computer scientists [4]. With 2048 node processors the peak performance of the CP-PACS is 614.4 GFLOPS. Intensive lattice QCD calculations on the CP-PACS have clarified the existence of quenched errors in the traditional calculations of light hadron spectrum in the quenched approximation [5], and opened the way towards precise full QCD calculations of hadronic quantities through the first systematic study of the light hadron spectrum with dynamical u,d quarks [6]. Our simulations of finite temperature QCD are based on the experiences of these zero-temperature studies.

2. FINITE TEMPERATURE QCD ON THE LATTICE

*Talk presented at *Statistical QCD*, Aug. 26–30, 2001, Bielefeld, Germany.

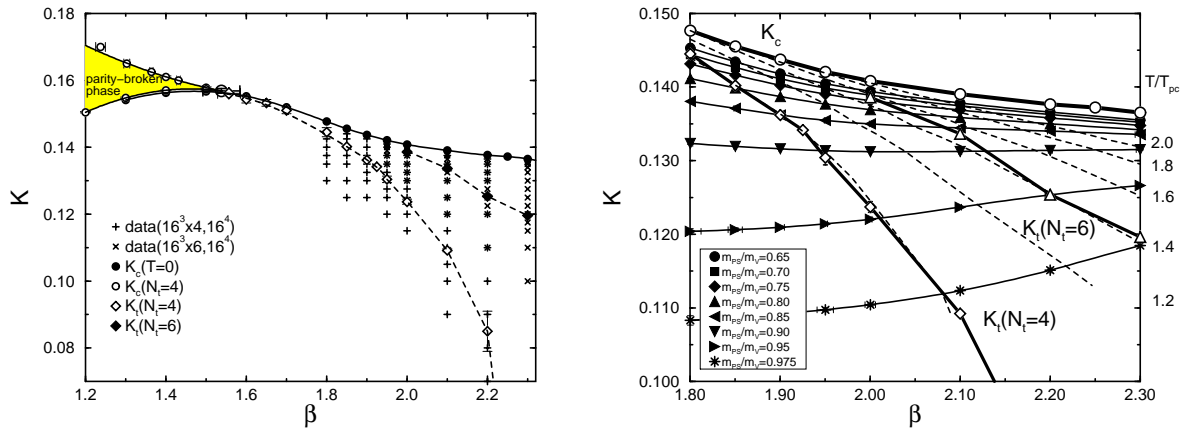


Figure 1. (a) Phase diagram and simulation points on $16^3 \times 4$, $16^3 \times 6$ and 16^4 lattices. (b) Lines of constant physics and of constant temperature. Solid lines are m_{PS}/m_V constant lines, and dashed lines are T/T_{pc} constant lines for $N_t = 4$. The values of T/T_{pc} for the dashed lines are given on the right edge of the figure. [2,3]

2.1. Lattice fermions

Until recently, EOS with dynamical quarks has been computed only with the Kogut-Susskind (staggered) type lattice fermions because of a smaller computational demand and persistence of a part of the chiral symmetry on the lattice [7]. The staggered fermion action, however, only allows four degenerate quark flavors, and the physically interesting cases of 2 and 2 + 1 flavors are simulated by artificially modifying a coefficient in the update algorithm, effectively introducing a non-local action. It has also been found that the critical scaling for two-flavor chiral transition extracted with this formalism does not reproduce the theoretically expected $O(4)$ critical exponents [8,9].

These problems of the staggered fermions make it imperative to study the issue with alternative lattice fermions — Wilson-type fermions or recently proposed lattice chiral fermions. The latter fermions, however, require too much computational cost on current computers to perform a systematic investigation over a wide range of the parameter space.

Wilson-type fermions have the manifest flavor symmetry and locality for any number of flavors. On the other hand, chiral symmetry is explicitly broken at finite lattice spacings, which complicates the phase diagram analysis on one hand and introduce sizable lattice artifacts on the other hand. Here, improvement of the lattice action was shown to be effective in reducing the lattice artifacts in finite temperature QCD [7]. In particular, the expected $O(4)$ scaling was observed around the two-flavor chiral transition [12].

From these observations, and also from a preparatory study of improved actions [13], we adopt an RG improved gauge action coupled with a clover-improved Wilson quark action, as in our zero-temperature full QCD simulations [6].

2.2. Phase diagram and lines of constant physics

Our simulation parameters are summarized in [2,3]. We study $N_t = 4$ and 6 lattices. The temperature is given by $T = 1/N_t a$, where we determine the lattice spacing a by the vector meson mass m_V at $T = 0$. Results for the phase diagram, together with the

simulation points for the EOS study, are summarized in Fig. 1(a). The horizontal axis is the inverse bare gauge coupling $\beta = 6/g^2$. The vertical axis, the hopping parameter K , corresponds to the freedom of the bare quark mass. The chiral limit is given by the $K_c(T = 0)$ line. The triangular region to the left, surrounded by the lines $K_c(N_t = 4)$, is the parity-flavor broken phase [10,11] for $N_t = 4$. Dashed lines K_t are the finite temperature pseudocritical lines for $N_t = 4$ (left) and 6 (right). which are determined by the peak position of the susceptibility for a Z(3)-rotated Polyakov loop.

In previous studies of EOS with staggered-type quark actions, the pressure and energy density are determined as functions of temperature for a fixed value of bare quark mass $m_q^{bare}a$ or $m_q^{bare}/T = m_q^{bare} N_t a$. While $m_q^{bare}a$ and N_t are practically easy to set in simulations, the results at different temperatures represent values for different physical systems with different renormalized quark masses. This is not useful for phenomenological applications; we want to see the temperature dependence of thermodynamic observables for a fixed physical system with fixed renormalized quark mass, *i.e.*, on a line of constant physics.

Therefore, it is important to evaluate the lines of constant physics also in finite temperature physics. Our results for the lines of constant physics, which are defined by fixed values of the ratio m_{PS}/m_V of the pseudo-scalar to vector meson masses at zero temperature, are summarized in Fig. 1(b) by solid lines. In the same figure, we also plot the lines of constant temperature normalized by the pseudocritical temperature T_{pc} at $K_t(N_t = 4)$ on the same line of constant physics.

3. RESULTS

3.1. Chiral transition temperature

We first study the chiral transition temperature T_c in the limit of massless quarks. In the phase diagram, Fig. 1(a), the chiral transition point is the crossing point of the chiral limit line $K_c(T = 0)$ and the finite temperature pseudocritical line K_t . We confirmed that the O(4) critical scaling, expected from an effective sigma model, is well satisfied with our data [2]. This implies that the chiral transition is second order in two-flavor QCD.

From a theoretical argument, we expect that the parity-broken phase at finite N_t locates in the low temperature phase [11]. This provides us with an estimate of the lower bound for the chiral transition point; $\beta_{ct} \geq 1.538(46)$ from the $K_c(N_t = 4)$ lines in Fig. 1(a). We can also estimate β_{ct} using the O(4) scaling properties of observables: From an O(4) fit to the chiral condensate, we find $\beta_{ct} = 1.469(73)$. On the other hand, from an O(4) scaling ansatz to the K_t line, we obtain $\beta_{ct} = 1.557(28)$. Collecting all the results, and converting to the physical units using the vector meson mass at $T = 0$, we obtain $T_c = 171 \pm 4$ MeV as our best estimate [2].

3.2. Equation of state

We calculate the pressure p by the integral method [14]. For the energy density ϵ , we combine the results for p and those for the interaction measure $\epsilon - 3p$ obtained by the differential method. Our results are shown in Fig. 2.

The continuum limit corresponds to the limit of large N_t . Our data show a 50% decrease from $N_t = 4$ to 6, both in the pressure and energy density, which is too large to attempt a continuum extrapolation. On $N_t = 6$ lattices, however, the magnitude and temperature

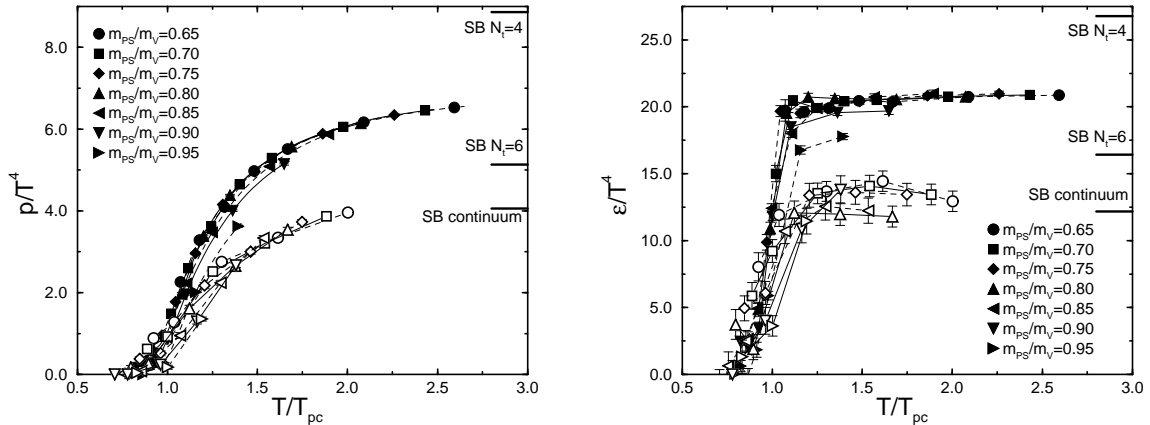


Figure 2. Pressure (a) and energy density (b) on $16^3 \times 4$ (filled symbols) and $16^3 \times 6$ (open symbols) lattices, as functions of T/T_{pc} [3].

dependence of the two quantities are quite similar between our improved Wilson quark action and the staggered quark action [15]. Together with the fact that the $N_t = 6$ results are close to the continuum SB limit at high temperatures, the approximate agreement of EOS between two different types of actions may be suggesting that the $N_t = 6$ results are not far from the continuum limit.

In Fig. 2, different values of m_{PS}/m_V correspond to different renormalized light quark masses. We find that the dependence on the quark mass is quite small for $m_{PS}/m_V \approx 0.65$ – 0.8 . A weak quark mass dependence appears only at $m_{PS}/m_V \gtrsim 0.9$ for $N_t = 4$ (the errors for the $N_t = 6$ data are still large to conclude a quark mass dependence). We find that the pressure and energy density in the quenched QCD ($m_{PS}/m_V = 1$) are much smaller [16]; only about $1/7$ of the values at $m_{PS}/m_V \sim 0.7$. See Figs. 15 and 17 of [3]. These results suggest that most dynamical quark effects are saturated between $m_{PS}/m_V = 1$ and 0.9 . Therefore, although the light u,d quark mass point, $m_{PS}/m_V = m_\pi/m_\rho = 1.8$, is still far away, our values for the EOS at $m_{PS}/m_V \sim 0.65$ – 0.8 may be already close to those at the physical point, except in the very vicinity of the chiral transition point where a singular limit according to the $O(4)$ critical exponents is expected.

This result of small quark mass dependence may not be surprising since hadron mass results in our zero-temperature simulations [6] show that the renormalized quark mass at $\mu = 2$ GeV in the \overline{MS} scheme at $m_{PS}/m_V \approx 0.65$ – 0.8 equals $m_q^{\overline{MS}}(\mu = 2\text{GeV}) \approx 100$ – 200 MeV, which is similar in magnitude to the critical temperature $T_c \approx 170$ MeV estimated for two-flavor QCD. For comparison, finite mass corrections for free fermion gas only amount to 7% when the temperature equals the fermion mass m_f , and exceed 50% only when $m_f/T \gtrsim 3$.

4. CONCLUSIONS

We have shown that a study of finite temperature QCD with Wilson-type quarks is feasible when improved lattice actions are adopted. Based on a systematic determination of the lines of constant physics, we calculate thermodynamic quantities in improved lattice

QCD with two flavors of Wilson-type quarks on $N_t = 4$ and 6 lattices, in the range $m_{\text{PS}}/m_V = 0.65\text{--}0.95$ and $T/T_c \lesssim 2.5$. We found that the quark mass dependence is small for $m_{\text{PS}}/m_V \lesssim 0.8$.

Concerning the continuum extrapolation, we find large scaling violations in EOS at $N_t = 4$, while $N_t = 6$ results are suggested to be not far from the continuum limit. Therefore, a precise continuum extrapolation may be possible from simulations at $N_t \gtrsim 6$. This is, however, computationally quite demanding. In this connection, I would like to introduce our recent study of EOS using anisotropic lattices [17]: We found that, in quenched QCD, anisotropic lattice is efficient to reduce discretization errors in EOS, such that a precise continuum extrapolation is possible with much smaller amount of computer time. Anisotropic lattices may help performing continuum extrapolations also in QCD with dynamical quarks.

The studies presented in this paper are performed by the CP-PACS Collaboration. This work is in part supported by the Grant-in-Aid of Ministry of Education, Science and Culture (Nos. 12304011 and 13640260).

REFERENCES

1. For an introduction of lattice QCD at finite temperatures, see K. Kanaya, Prog. Theor. Phys. Suppl. 131 (1998) 73.
2. A. Ali Khan *et al.* (CP-PACS Collaboration), Phys. Rev. D63 (2001) 034502.
3. A. Ali Khan *et al.* (CP-PACS Collaboration), Phys. Rev. D64 (2001) 074510.
4. The CP-PACS Project has been described in Y. Iwasaki, Nucl. Phys. B (Proc. Suppl.) 60A (1998) 246; T. Boku *et al.*, “CP-PACS: A massively parallel processor for large scale scientific calculations”, in Proc. Supercomputing '97 (1997) 108. For further details, see <http://www.rccp.tsukuba.ac.jp>.
5. S. Aoki *et al.* (CP-PACS Collaboration), Phys. Rev. Lett. 84 (2000) 238; full paper in preparation.
6. A. Ali Khan *et al.* (CP-PACS Collaboration), Phys. Rev. Lett. 85 (2000) 4671; hep-lat/0105015 (2001).
7. For a recent review, see S. Ejiri, Nucl. Phys. B (Proc. Suppl.) 94 (2000) 19.
8. S. Aoki *et al.*, Phys. Rev. D57 (1998) 3910.
9. E. Laermann, Nucl. Phys. B (Proc. Suppl.) 60A (1998) 180.
10. S. Aoki, Phys. Rev. D30 (1984) 2653; Phys. Rev. Lett. 57 (1986) 3136; Nucl. Phys. B314 (1989) 79.
11. S. Aoki *et al.*, Phys. Rev. Lett. 76 (1996) 873; S. Aoki *et al.*, Nucl. Phys. B (Proc. Suppl.) 63 (1998) 397.
12. Y. Iwasaki, K. Kanaya, S. Kaya and T. Yoshié, Phys. Rev. Lett. 78 (1997) 179.
13. S. Aoki *et al.* (CP-PACS Collaboration), Phys. Rev. D60 (1999) 114508.
14. J. Engels *et al.*, Phys. Lett. B252 (1990) 625.
15. C. Bernard *et al.*, Phys. Rev. D55 (1997) 6861.
16. M. Okamoto *et al.* (CP-PACS Collaboration), Phys. Rev. D60 (1999) 094510.
17. Y. Namekawa *et al.* (CP-PACS Collaboration), Phys. Rev. D64 (2001) 074507.